Published in final edited form as:
Neuroscience. 2014 September 5; 275: 305–313. doi:10.1016/j.neuroscience.2014.06.022.

Circadian cycle dependent EEG biomarkers of pathogenicity in adult mice following prenatal exposure to *in utero* inflammation

Daniel A Adler[1,5], **Simon Ammanuel**[1,5], **Jun Lei**[4], **Tahani Dada**[4], **Talaibek Borbiev**[4], **Michael.V. Johnston**[1,2,3], **Shilpa.D. Kadam**[1,2], and **Irina Burd**[2,4]

[1]Departments of Neuroscience, Hugo Moser Research Institute at Kennedy Krieger, Johns Hopkins University, Baltimore, MD, USA 21205

[2]Department of Neurology, Johns Hopkins University, Baltimore, MD, USA 21205

[3]Department of Pediatrics, Johns Hopkins University, Baltimore, MD, USA 21205

[4]Integrated Research Center for Fetal Medicine, Departments of Gynecology and Obstetrics, Johns Hopkins University, Baltimore, MD, USA 21205

[5]Department of Biomedical Engineering, Johns Hopkins University, Baltimore, MD, USA 21205

Abstract

Intrauterine infection or inflammation in preterm neonates is a known risk for adverse neurological outcomes, including cognitive, motor and behavioral disabilities. Our previous data suggest that there is acute fetal brain inflammation in a mouse model of intrauterine exposure to lipopolysaccharides (LPS). We hypothesized that the *in utero* inflammation induced by LPS produces long-term EEG biomarkers of neurodegeneration in the exposed mice that could be determined by using continuous quantitative video-EEG-EMG analyses. A single LPS injection at E17 was performed in pregnant CD1 dams. Control dams were injected with same volumes of saline (LPS n=10, Control n=8). At postnatal age of P90-100, 24h synchronous video/EEG/EMG recordings were done using a tethered recording system and implanted subdural electrodes. Behavioral state scoring was performed blind to treatment group, on each 10 second EEG epochs using synchronous video, EMG and EEG trace signatures to generate individual hypnograms. Automated EEG power spectrums were analyzed for delta and theta-beta power ratios during wake vs. sleep cycles. Both control and LPS hypnograms showed an ultradian wake/sleep cycling. Since rodents are nocturnal animals, control mice showed the expected diurnal variation with significantly longer time spent in wake states during the dark cycle phase. In contrast, the LPS treated mice lost this circadian rhythm. Sleep microstructure also showed significant alteration in the LPS mice specifically during the dark cycle, caused by significantly longer average NREM cycle durations. No significance was found between treatment groups for the delta power data;

Corresponding Authors: Shilpa D. Kadam, PhD, 716 North Broadway, # 426, Baltimore MD 21205, Phone: 443-923-2688, Fax: 443-923-2695, kadam@kennedykrieger.org. Irina Burd, MD. PhD, Integrated Research Center for Fetal Medicine, Department of Gynecology and Obstetrics, 600 North Wolfe Street, Phipps 228, Baltimore, MD 20905, Phone: 410-955-8496, iburd1@jhmi.edu.

however, significant activity dependent changes in theta-beta power ratios seen in controls were absent in the LPS-exposed mice. In conclusion, exposure to *in utero* inflammation in CD1 mice resulted in significantly altered sleep architecture as adults that were circadian cycle and activity state dependent.

Keywords

LPS - Lipopolysaccharide; qEEG - quantitative electroencephalogram; EMG- electromyogram; prenatal maternal infection; circadian; TBR - theta beta ratio

1. Introduction

Recent research is finding an increasing connection between prenatal brain inflammation and many adult onset neurodegenerative and psychiatric disorders (Boksa, 2013;Harvey and Boksa, 2012;Boksa, 2008). Evidence suggests a correlation between inflammatory responses *in utero* and later onset epilepsy, Parkinson's disease, attention deficit hyperactivity disorder (ADHD), Alzheimer's disease, and recently autism spectrum disorders (ASD) (Deleidi and Gasser, 2013;Donev and Thome, 2010;Strohmeyer and Rogers, 2001;Theoharides et al., 2013;Vezzani et al., 2013). It is theorized that fetal infection/inflammation may underlie the pathogenesis of pre-term brain injury. This results in the deregulation of many key cytokines and chemokines including interleukin-1 (IL-1), IL-6, and tumor necrosis factor alpha (TNFα) (Mayer et al., 2013).

The endotoxin lipopolysaccharide (LPS) has gained attention as a possible tool to mimic prenatal brain inflammation leading to neurological deficits and chronic brain inflammation in adulthood (Dada et al., 2014). LPS is a component of the outer-membrane of Gram-negative bacteria. At critical concentrations of LPS, the immune system initiates a rapid rise in pro-inflammatory molecules including IL-1, IL-6 and TNFα (Chorawala et al., 2013). It has also been reported that a single LPS injection postnatally can result in brain TNFα production that continues for months after the need for an inflammatory-response has diminished, leading to the destruction of dopaminergic (DA) neurons (Chorawala et al., 2013). Furthermore, mice injected with LPS postnatally have also been found to exhibit behavioral patterns that are associated with anxiety and depression (Barnum et al., 2012;Dantzer, 2006). Therefore, the LPS model can help investigate mechanisms underlying many neurodegenerative disorders (Qin et al., 2007).

One simple method that is becoming more effective in diagnosing many neurodegenerative and neuropsychiatric disorders is electroencephalogram/electromyogram (EEG/EMG) recordings. Quantitative EEG allows delineating objective biomarkers in contrast to the subjective quality of quantitating behavior-related disorders like depression and anxiety (Chen et al., 1995;Steiger and Kimura, 2010). Recently, EEG power analysis has also been shown to be a valid biomarker for ADHD, evident by an increase in the average theta-beta power ratio [TBR (Arns et al., 2013)]. In addition, the *postnatal* LPS model has been reported to show an increase in the delta-power spectra intensity in hamsters, and in effect a higher intensity of non-rapid eye movement sleep [i.e.; NREM (Ashley et al., 2012)].

Currently, there are no well-defined qualitative or quantitative EEG biomarkers to the behavioral phenotype associated with *in utero* exposure to LPS mouse model. In these studies, we tested the hypothesis that mice exposed to LPS *in utero* would produce chronic EEG biomarkers associated with the prenatal brain inflammation as adults. These biomarkers could then be used to quantitatively evaluate phenotype severity and modulation by early postnatal interventions.

2. Methods

All animal care and treatment procedures were approved by the Institutional Animal Care and Use Committee. Animals were handled according to the National Institutes of Health guidelines. An established model of intrauterine inflammation was utilized for these studies (Burd et al., 2011;Elovitz et al., 2011;Burd et al., 2012;Leitner et al., 2014;Dada et al., 2014). Timed pregnant CD1 outbred mouse strain was obtained from Charles River Laboratories (Wilmington, MA).

2.1 Animals and Treatments

All mice underwent prenatal surgery per our previously described protocol (Leitner et al., 2014;Dada et al., 2014). Briefly following induction of anesthesia, a mini-laparotomy was performed. Intrauterine injections of LPS (from Escherichia coli, 055: B5, Sigma-Aldrich, St Louis, MO) at a dose of 50μg in 100 μL of phosphate-buffered saline (PBS) were administered on embryonic day 17 of a 19-day gestation. Control dams for these experiments received the same volume of intrauterine injection of vehicle phosphate buffered solution (PBS; control). The results produced 10 LPS experimental mice and 8 control mice, each representing different litters. At postnatal day (PND) 21 days, the mice were weaned and brought into experimentation after maturing for three months.

2.2 EEG Surgery

The mice that underwent EEG recording were housed in the animal facilities at Johns Hopkins Medical Institutions with a standard 12-hour light on/off cycle with food and water available ad-lib. These facilities meet Federal and NIH regulations for animal care and are currently accredited by the American Association for Accreditation of Laboratory Animal Care. All animal experimentation was conducted in accordance with protocols approved by the guidelines of the Johns Hopkins AACUC. The LPS exposed mice (n=10, 5 male, 5 female) and saline control mice (n=8, 3 male, 5 female) used in this study were all aged between 90–100 days old. Under general anesthesia, mice were surgically implanted with electroencephalogram (EEG; subdural) and electromyogram (EMG; suprascapular) recording electrodes using coordinates from bregma (see Figure 1B) modified from a similar previous rat protocol designed for continuous EEG using a head mount (Kadam et al., 2010).

2.3 24 Hour EEG/EMG Recording

After recovery from surgery (3–6 days), EEG and EMG waveforms along with video were recorded for an entire 24 hour light-dark cycle using a tethered pre-amplifier and commutator that allowed free movement within recording chamber and unrestricted access to food and water. Each mouse received a small piece of bedding from its own home cage in

addition to a new piece of bedding material. EEG and EMG waveforms were recorded and analyzed using the 8400 system recording system and Sirenia sleep software package (Pinnacle Technology Inc., Lawrence, KS).

2.4 Sleep Analysis

All recorded EEG waveforms were scored as 10-second epochs of wake (W: high frequency low amplitude, high EMG activity), non-rapid eye movement (NREM: low frequency, high amplitude (i.e.; slow wave activity), silent EMG) or rapid eye movement (REM: high frequency, low amplitude (i.e.; paradoxical sleep) and silent EMG with occasional activity) sleep by a blinded scorer. Criteria for scoring were based upon a combination of wave amplitude and frequency, as well as synchronous EMG and video for confirmation of wake-inactive states (Brankack et al. 2010). After scoring, power data, spectral plots, and hypnograms were extracted as well as the duration, percentage, and cycle counts for each sleep type (Figure 2). Scoring was compared against power data for consistency before un-blinding. Also, the nesting cycle (wake cycle in which mouse creates their nest from given bedding material) was extracted for duration as well as the latency to first sleep.

2.5 Power Analysis

Power data extracted from the EEG1 lead for each mouse was analyzed. Data was separated into delta (0.5–4.0 Hz), theta (5.5–8.0 Hz), alpha (8.0–13.0 Hz), beta (13.0–30.0 Hz) and gamma (35–44 Hz) waveforms. To compare the total delta power during the 24-hour period, we proposed using area under the curve (AUC) analysis with delta power vs. time graphs. The delta-power AUC was calculated for the sleep and wake cycles of each mouse with trapezoidal summations using R statistical software (R Core Team 2013, Trapletti and Hornik 2013, Wickham 2011, Ekstrom 2013, Zeileis and Grothendieck 2005, Borchers 2013, Liland and Mevik 2013, Komsta 2011). The data was cleaned by separating the sleep and wake delta power and filtered by removing points 2.5 deviations away from the average delta power in a set window of 200 10-second epochs. The sleep and wake files were then concatenated. The AUC was analyzed during the transition periods for sleep cycles greater than ten minutes. The first ten minutes of the sleep cycle were isolated, and the preceding ten minutes of wake before the cycle were isolated. The AUC was then calculated for the sleep transition and its preceding wake, and the data was normalized by dividing the ten minutes of sleep AUC by its preceding wake AUC. To verify this data, average power data for 1 Hz, 2 Hz, and 4 Hz (delta power) was extracted from each mouse for NREM and wake cycles. The NREM power at each of these frequencies was then divided by the corresponding wake power to provide a ratio. The theta-beta ratio (TBR) was calculated by dividing theta power at each epoch by its corresponding beta power: TBR= Theta power/ beta power. Averages were calculated for the TBR during the total 24 hours, total wake, total sleep, as well as the sleep wake during the light and dark periods.

2.6 Statistical Analysis

All values are expressed as mean ± standard error (SE). Differences were calculated using independent t-tests between the LPS and control groups. Paired t-tests within groups were also calculated, as well as correlations. The null hypothesis in each test was rejected at α=0.05.

3. Results

3.1 Circadian rhythm dependent sleep analysis

Scored sleep cycles were tested for mean duration of wake, sleep, NREM and REM as well as the percentage of Sleep, Wake NREM and REM during the entire recording, light and dark cycles (Figure 3). No significance was found during the light cycle between the wake for controls (52±4%) and LPS (53±2%), and the sleep for controls (48±3%) and LPS (47±2%). During the dark cycle, significance was found within the wake (64±2%) and sleep (36±2%) for control mice (n=8, p=0.001), but not between the wake (54±3%) and sleep (46±3%) for LPS mice. In addition, a significant difference was found within the controls between percentage light and percentage dark wake (n=8, p=0.024), and between percentage light and percentage dark sleep (n=8, p=0.024). This significance was not found within the LPS mice. Controls and LPS were found to have a significance difference between the wake (n=18, p=0.039) and sleep (n=18, p=0.039). During the light cycle, no significance was found between the average NREM (497±55sec) and REM (86±5sec) cycle duration for control mice, and average NREM (479±35sec) and REM cycle duration (85±4sec) for LPS mice. Significance was found in the dark cycle between the average NREM cycle duration for control (328±24sec) and LPS (390±16sec) mice (n=18, p=0.043), but not between control REM (96±4sec) and LPS REM (84±6sec) duration. Therefore, between groups significance for circadian rhythm analysis was only found during the dark cycle.

3.2 Delta power sleep/wake transition area under the curve (AUC) analysis

Delta power area under the curve was analyzed after calculating the sleep/wake ratios. In addition, the quadratic correlation was analyzed using the coefficient of determination (Figure 4). The sleep/wake ratios for controls (16±5) compared to LPS (12±2) mice were not significant during the light cycle. The same was found during the dark cycle for controls (14±3) and LPS (15±2). No significance was found between control (0.35±0.080) and LPS (0.23±0.079) mice for the quadratic coefficient of determination. In summary, delta power AUC did not differ significantly, but control delta power appeared to have a parabolic change over time during the 24-hour cycle though this trend was not significantly different between LPS and controls.

3.3 Theta-beta ratio analysis

Theta-beta power ratios (TBR) were calculated and analyzed during each of the light and dark periods (Figure 5). Significance was found within controls during wake (0.74±0.085) and sleep (0.87±0.096) for the light cycle (n=8, p=0.022), as well as wake (0.74±0.10) and sleep (0.90±0.10) for the dark cycle (n=8, p=0.036). No significance was found within the LPS mice group during wake (0.82±0.010) and sleep (0.92±0.080) in the light cycle or during wake (0.90±0.11) and sleep (0.95±0.063) during the dark cycle. Control mice differed between their wake and sleep TBR during both cycles, while LPS mice did not show this same trend due to a higher TBR during the wake cycles.

3.4 Nesting Cycle analysis

The nesting cycle (Figure 6) duration and latency until first sleep were recorded. No significance was found for the nesting cycle between controls (10149±853sec) and LPS (7588±1571) and for sleep latency between controls (6814±1477sec) and LPS (7260±607).

3.5 Male vs. female analysis

The data was re-analyzed by sex to investigate the sex differences associated with this prenatal brain inflammation for their EEG biomarkers. Significance was found between the control (102±3sec) and LPS (79±7sec) average dark phase REM cycle durations (n=5 each, p=0.017) in females that was absent in males (control 86±6sec and LPS 88±8,5sec). No other sex differences were found.

4. Discussion

This study, for the first time reports the sleep architecture and EEG spectral power alterations in adult mice following exposure to a prenatal inflammation. The novel findings of this study are 1. LPS mice had a significantly longer time spent in sleep states during the dark cycle compared to controls. 2. This alteration was driven by significantly longer average NREM cycle durations during the dark cycle in the LPS mice. None of these findings were found to be significant between the LPS and control mice during the light cycle for either their wake or sleep cycles during the 24h recordings. 3. Delta power analysis did reveal that the control mice sleep/wake ratios followed a quadratic model throughout the 24h circadian cycle that was abolished in the LPS mice; however the difference was not significant between the two treatment groups. 4. Lastly, TBR was significantly different between wake and sleep states for both the light and dark cycle in control mice; this significance was lost in the LPS exposed mice. In summary, the prenatal LPS exposure resulted in circadian cycle and activity state dependent alterations in sleep structure. These alterations that were restricted to the dark cycle in the LPS mice highlight the significance of a 24h monitoring protocol. Our hypothesis for this study was that we would detect biomarkers of neurodegeneration using qEEG at PND100, and it was based on our observations of chronic inflammation in adult brain of mice with history of prenatal exposure to inflammation (Dada et al., 2014). This study reports the identified biomarkers. Our future studies will address qEEG biomarkers at earlier postnatal periods in order to identify and quantify changes following early postnatal interventions.

4.1 Long-term co-morbidity associated with prenatal LPS exposure and translational value

Infection and inflammation during pregnancy remain a significant contributor to infant morbidity and a known spectrum of long-term adverse neurobehavioral outcomes, including cerebral palsy cognitive delay, schizophrenia, autism and mental retardation. However, majority of sequelae are known to occur in presence of intrauterine inflammation, even in the absence of infection. Understanding this more common clinical scenario, we have utilized a mouse model that accurately mimics intrauterine inflammation in the human. More recently, we have demonstrated in this model that exposure to intrauterine inflammation results in postnatal brain injury, with chronic inflammation, presence of macrophages within adult cortex and activation of microglia (Leitner et al., 2014;Dada et al.,

2014). The findings of this study suggest that exposure to prenatal inflammation alone may lead to neurodegenerative diseases; these changes may be related to increased number of macrophages in the exposed adult brains and the presence of activated microglia. Translational interpretations for the findings of this study reported above would indicate that the model aligns with neurodegenerative syndromes associated with increased and abnormal sleep during the day (the mice are nocturnal) and an impaired “internal body clock” in patients. Recent literature has associated LPS exposure models to represent Alzheimer’s Tau pathophysiology (Kitazawa et al., 2005). Additionally, systemic immune challenges during the gestational age have been shown to induce Alzheimer-like neuropathology in mice (Krstic et al., 2012;Knuesel, 2011;Harvey and Boksa, 2012). In our previous studies in this model, we have documented long-term chronic inflammation and neurologic deficits, behavioral and structural (Dada 2014).

Our findings in the prenatally exposed LPS CD1 mice is supported by similar diurnal variations reported in 24h EEGs from adult mice exposed to LPS via IP injections (Morrow and Opp, 2005). Based on the finding of a reduction of GAD-67 positive cells in the hippocampi of prenatally LPS exposed rats, previous reports have compared their models to represent that of possible contributors to the pathophysiology of schizophrenia or autism in humans. However, sleep cycle disturbances in autism have been reported as defined by extreme sleep latencies; lengthy periods of night waking; shortened night sleep; and early morning waking. None of these findings were seen with the 24 EEG following LPS in adult mice or in our study. Acute post-LPS recordings however have shown an age-dependent effect on sleep structure when comparing young and old rats (Schiffelholz and Lancel, 2001) that may not apply to models of intrauterine exposure/inflammation and are therefore distinct.

The sleep cycle and circadian cycle dysfunction are well described and quantitated for Alzheimer’s disease (Ju et al., 2014;Musiek et al., 2013;Roh et al., 2012;Steiger and Kimura, 2010;Strohmeyer and Rogers, 2001). Additionally, sleep-wake cycles themselves directly influence levels of Aβ in the brain (Ju et al., 2014) and has been proposed as a predictor of Alzheimer’s disease (Hita-Yanez et al., 2013). Daytime sleepiness is the hallmark of certain dementias especially Alzheimer’s (Bonanni et al., 2005) and recapitulates the dark-cycle sleep dominance in the prenatal LPS model. Disturbances of slow wave sleep which identifies the NREM cycles have been reported to altered in dementia patients and genetic rodent models of Alzheimer’s (Jyoti et al., 2010). The prenatal LPS model also showed significant alterations in NREM sleep during the dark cycle in this study.

4.2 EEG and associated adult behavioral and imaging phenotypes in the prenatal LPS model

The recently reported LPS-induced behavioral and imaging phenotypes in adult mice with prenatal LPS exposure (Dada et al., 2014) have shown profiles of significantly increased peripheral activity in the open-field test and significantly atrophied hippocampi at PND 60. The imaging data were specific for hippocampal atrophy but the overall brain volumes for neocortex and deep gray matter remained unaltered. Clinical studies have similarly reported

significantly smaller hippocampal volumes in patients with memory deficits diagnosed with Alzheimer's and the results were also mildly associated with worse memory scores (Ferrarini et al., 2014). The current study qEEG findings add additional insight into the prenatal LPS model by characterizing the sleep structure underlying these behavioral and anatomical phenotypes. Although correlations are not possible with the current study between the behavioral and EEG characteristics, the findings of this study will help design future protocols that help ask those specific questions.

4.3 Relevance of sleep delta power and TBR in models of *in utero* inflammation

Quantitative spectral EEGs are now being regularly used to identify diagnostic and prognostic markers in neurodegenerative diseases associated with dementia (Claus et al., 1998;Poza et al., 2008). Slow wave activity during NREM (i.e.; delta spectral power) identifies and quantitates the quality of sleep and has significant implications for long-term memory consolidation during sleep cycles. This study showed that the ratios of delta power during NREM normalized to the preceding wake state showed diurnal changes over the 24h cycle in control mice that were lost in the LPS treated mice. This loss of diurnal variation occurred due to the dark cycle exacerbation of delta power during the significantly longer NREM cycles.

However, the study failed to show significance in these differences, which likely originated from the variability in the severity of the *in utero* insult between pups from different litters (i.e.; LPS mice that showed delta power similar to controls, see figure 4H). Significantly increased delta power has been reported in Alzheimer's patients (Poza et al., 2008). The findings of the Poza et al., studies not only indicate that spectral ratios could be useful descriptors to help in diagnosis but also correlate significantly with the severity of dementia. The group data in this mouse model study did not reach significance due to two LPS mice that had delta power dynamics similar to controls; these may have represented non-symptomatic mice. However future studies where experiments designed to be able to directly correlate behavior, imaging and EEG will be able better to address that question.

TBR ratios derived using single-channel quantitative EEG have recently been in the spotlight in autism research (Chan and Leung, 2006) and have been proposed to underlie impaired connectivity associated with the ADHD symptoms in autistic children. The novel finding of the loss of activity dependent modulation of TBR ratios reported for this LPS model (see Fig. 5) highlights the importance of this qEEG biomarker in neurodevelopmental disorders.

4.4 Conclusion

This is the first report of 24h qEEG in adult mice prenatally exposed to LPS. The 24h EEG allowed the identification and quantification of dark cycle specific biomarkers of activity-state dependent pathophysiology that can now be used to correlate with the behavioral phenotypes, hippocampal atrophy and histological studies in the future. EEG is now regularly being used in prognostication of progressive nervous system disorders and it is imperative that animal models of human conditions that lead long-term neurological sequelae do the same.

Acknowledgments

This work was supported by Aramco Services Company Fund (IB), NICHD K08HD073315 (IB), NINDS-NS28208 (MJ).

Reference List

Arns M, Conners CK, Kraemer HC. A Decade of EEG Theta/Beta Ratio Research in ADHD: A Meta-Analysis. Journal of Attention Disorders. 2013; 17:374–383. [PubMed: 23086616]

Ashley NT, Zhang N, Weil ZM, Magalang UJ, Nelson RJ. Photoperiod alters duration and intensity of non-rapid eye movement sleep following immune challenge in Siberian hamsters (Phodopus sungorus). Chronobiol Int. 2012; 29:683–692. [PubMed: 22734569]

Barnum CJ, Pace TW, Hu F, Neigh GN, Tansey MG. Psychological stress in adolescent and adult mice increases neuroinflammation and attenuates the response to LPS challenge. J Neuroinflammation. 2012; 9:9. [PubMed: 22248083]

Boksa P. Maternal infection during pregnancy and schizophrenia. J Psychiatry Neurosci. 2008; 33:183–185. [PubMed: 18592037]

Boksa P. A way forward for research on biomarkers for psychiatric disorders. J Psychiatry Neurosci. 2013; 38:75–77. [PubMed: 23422052]

Bonanni E, Maestri M, Tognoni G, Fabbrini M, Nucciarone B, Manca ML, Gori S, Iudice A, Murri L. Daytime sleepiness in mild and moderate Alzheimer's disease and its relationship with cognitive impairment. J Sleep Res. 2005; 14:311–317. [PubMed: 16120107]

Burd I, Brown A, Gonzalez JM, Chai J, Elovitz MA. A mouse model of term chorioamnionitis: unraveling causes of adverse neurological outcomes. Reprod Sci. 2011; 18:900–907. [PubMed: 21421895]

Burd I, Balakrishnan B, Kannan S. Models of Fetal Brain Injury, Intrauterine Inflammation, and Preterm Birth. Am J Reprod Immunol. 2012; 67:287–294. [PubMed: 22380481]

Chan AS, Leung WWM. Differentiating Autistic Children with Quantitative Encephalography: A 3-Month Longitudinal Study. Journal of Child Neurology. 2006; 21:391–399. [PubMed: 16901444]

Chen LS, Mitchell WG, Horton EJ, Snead OC III. Clinical utility of video-EEG monitoring. Pediatr Neurol. 1995; 12:220–224. [PubMed: 7619188]

Chorawala MR, Oza PM, Trivedi VR, Deshpande SS, Shah GB. Lipopolysacchardies: An Overview. World Journal of Pharmacy and Pharmaceutical Sciences. 2013; 2:465–477.

Claus JJ, Ongerboer de Visser BW, Walstra GM, Hijdra A, Verbeeten B, Jr, van Gool WA. QUantitative spectral electroencephalography in predicting survival in patients with early alzheimer disease. Archives of Neurology. 1998; 55:1105–1111. [PubMed: 9708961]

Dada T, Rosenzweig JM, Al SM, Firdaus W, Al RS, Borbiev T, Tekes A, Zhang J, Alqahtani E, Mori S, Pletnikov MV, Johnston MV, Burd I. Mouse model of intrauterine inflammation: Sex-specific differences in long-term neurologic and immune sequelae. Brain Behav Immun. 2014

Dantzer R. Cytokine, sickness behavior, and depression. Neurol Clin. 2006; 24:441–460. [PubMed: 16877117]

Deleidi M, Gasser T. The role of inflammation in sporadic and familial Parkinson's disease. Cell Mol Life Sci. 2013; 70:4259–4273. [PubMed: 23665870]

Donev R, Thome J. Inflammation: good or bad for ADHD? Atten Defic Hyperact Disord. 2010; 2:257–266. [PubMed: 21432611]

Elovitz MA, Brown AG, Breen K, Anton L, Maubert M, Burd I. Intrauterine inflammation, insufficient to induce parturition, still evokes fetal and neonatal brain injury. Int J Dev Neurosci. 2011; 29:663–671. [PubMed: 21382466]

Ferrarini L, van Lew B, Reiber JHC, Gandin C, Galluzzo L, Scafato E, Frisoni GB, Milles J, Pievani M. Hippocampal atrophy in people with memory deficits: results from the population-based IPREA study. International Psychogeriatrics FirstView. 2014:1–15.

Harvey L, Boksa P. Prenatal and postnatal animal models of immune activation: relevance to a range of neurodevelopmental disorders. Dev Neurobiol. 2012; 72:1335–1348. [PubMed: 22730147]

Hita-Yanez E, Atienza M, Cantero JL. Polysomnographic and subjective sleep markers of mild cognitive impairment. Sleep. 2013; 36:1327–1334. [PubMed: 23997365]

Ju YE, Lucey BP, Holtzman DM. Sleep and Alzheimer disease pathology-a bidirectional relationship. Nat Rev Neurol. 2014; 10:115–119. [PubMed: 24366271]

Jyoti A, Plano A, Riedel G, Platt B. EEG, activity, and sleep architecture in a transgenic AbetaPPswe/PSEN1A246E Alzheimer's disease mouse. J Alzheimers Dis. 2010; 22:873–887. [PubMed: 20858963]

Kadam SD, White AM, Staley KJ, Dudek FE. Continuous Electroencephalographic Monitoring with Radio-Telemetry in a Rat Model of Perinatal Hypoxia-Ischemia Reveals Progressive Post-Stroke Epilepsy. J Neurosci. 2010; 30:404–415. [PubMed: 20053921]

Kitazawa M, Oddo S, Yamasaki TR, Green KN, LaFerla FM. Lipopolysaccharide- Induced Inflammation Exacerbates Tau Pathology by a Cyclin-Dependent Kinase 5- Mediated Pathway in a Transgenic Model of Alzheimer's Disease. The Journal of Neuroscience. 2005; 25:8843–8853. [PubMed: 16192374]

Knuesel I. [Prenatal infection as driving force of aging-associated neurodegenerative diseases]. Praxis (Bern 1994). 2011; 100:299–304. [PubMed: 21365561]

Krstic D, Madhusudan A, Doehner J, Vogel P, Notter T, Imhof C, Manalastas A, Hilfiker M, Pfister S, Schwerdel C, Riether C, Meyer U, Knuesel I. Systemic immune challenges trigger and drive Alzheimer-like neuropathology in mice. J Neuroinflammation. 2012; 9:151. [PubMed: 22747753]

Leitner K, Al SM, McLane M, Johnston MV, Elovitz MA, Burd I. IL-1 Receptor Blockade Prevents Fetal Cortical Brain Injury but Not Preterm Birth in a Mouse Model of Inflammation-Induced Preterm Birth and Perinatal Brain Injury. Am J Reprod Immunol. 2014

Mayer CL, Huber BR, Peskind E. Traumatic brain injury, neuroinflammation, and post-traumatic headaches. Headache. 2013; 53:1523–1530. [PubMed: 24090534]

Morrow JD, Opp MR. Diurnal variation of lipopolysaccharide-induced alterations in sleep and body temperature of interleukin-6-deficient mice. Brain, Behavior, and Immunity. 2005; 19:40–51.

Musiek ES, Lim MM, Yang G, Bauer AQ, Qi L, Lee Y, Roh JH, Ortiz-Gonzalez X, Dearborn JT, Culver JP, Herzog ED, Hogenesch JB, Wozniak DF, Dikranian K, Giasson BI, Weaver DR, Holtzman DM, Fitzgerald GA. Circadian clock proteins regulate neuronal redox homeostasis and neurodegeneration. J Clin Invest. 2013; 123:5389–5400. [PubMed: 24270424]

Poza J, Hornero R, Abasolo D, Fernandez A, Mayo A. Evaluation of spectral ratio measures from spontaneous MEG recordings in patients with Alzheimer's disease. Comput Methods Programs Biomed. 2008; 90:137–147. [PubMed: 18249462]

Qin L, Wu X, Block ML, Liu Y, Breese GR, Hong JS, Knapp DJ, Crews FT. Systemic LPS causes chronic neuroinflammation and progressive neurodegeneration. Glia. 2007; 55:453–462. [PubMed: 17203472]

Roh JH, Huang Y, Bero AW, Kasten T, Stewart FR, Bateman RJ, Holtzman DM. Disruption of the sleep-wake cycle and diurnal fluctuation of beta-amyloid in mice with Alzheimer's disease pathology. Sci Transl Med. 2012; 4:150ra122.

Schiffelholz T, Lancel M. Sleep changes induced by lipopolysaccharide in the rat are influenced by age. American Journal of Physiology - Regulatory, Integrative and Comparative Physiology. 2001; 280:R398–R403.

Steiger A, Kimura M. Wake and sleep EEG provide biomarkers in depression. J Psychiatr Res. 2010; 44:242–252. [PubMed: 19762038]

Strohmeyer R, Rogers J. Molecular and cellular mediators of Alzheimer's disease inflammation. J Alzheimers Dis. 2001; 3:131–157. [PubMed: 12214082]

Theoharides TC, Asadi S, Patel AB. Focal brain inflammation and autism. J Neuroinflammation. 2013; 10:46. [PubMed: 23570274]

Vezzani A, Aronica E, Mazarati A, Pittman QJ. Epilepsy and brain inflammation. Exp Neurol. 2013; 244:11–21. [PubMed: 21985866]

Glossary

Circadian Rhythm	Any biological process that oscillates in a 24 hour cycle. The 24- hour sleep/wake cycle is a common circadian-dependent biological process in animals. Mice commonly follow a nocturnal circadian-dependent cycle (longer duration of wake during day, sleep at night)
Diurnal Variation	Variation that is day/night dependent
in utero	Any procedure taking place in the womb
Lipopolysaccharides (LPS)	Endotoxin found on the outer membrane of Gram-negative bacteria. At high levels of LPS, the immune system initiates a rapid rise in proinflammatory molecules including IL-1, IL-6 and TNFα
Nesting Cycle	Wake cycle in which mice create a nest from given bedding material. Each mouse was given a single square piece of bedding at the beginning of each EEG/EMG recording
Non-rapid eye movement sleep (NREM)	Sleep characterized by high amplitude, low frequency waveforms
Rapid eye movement sleep (REM)	Sleep characterized by low amplitude, high freqeuncy waveforms
Sleep Power	Measure of EEG activity during sleep. Power is split into delta (0.5–4.0 Hz), theta (5.5–8.0 Hz), alpha (8.0–13.0 Hz), beta (13.0–30.0 Hz) and gamma (35–44 Hz) waveforms

Highlights

1. EEG biomarkers of circadian cycle dependent sleep alterations in LPS mice.
2. qEEG with synchronous EMG recordings used as a novel approach.
3. Quantitative 24h EEG identifies night-cycle specific sleepiness.
4. Sleep microstructure evaluation identify NREM alterations.
5. Activity dependent modulation of TBR

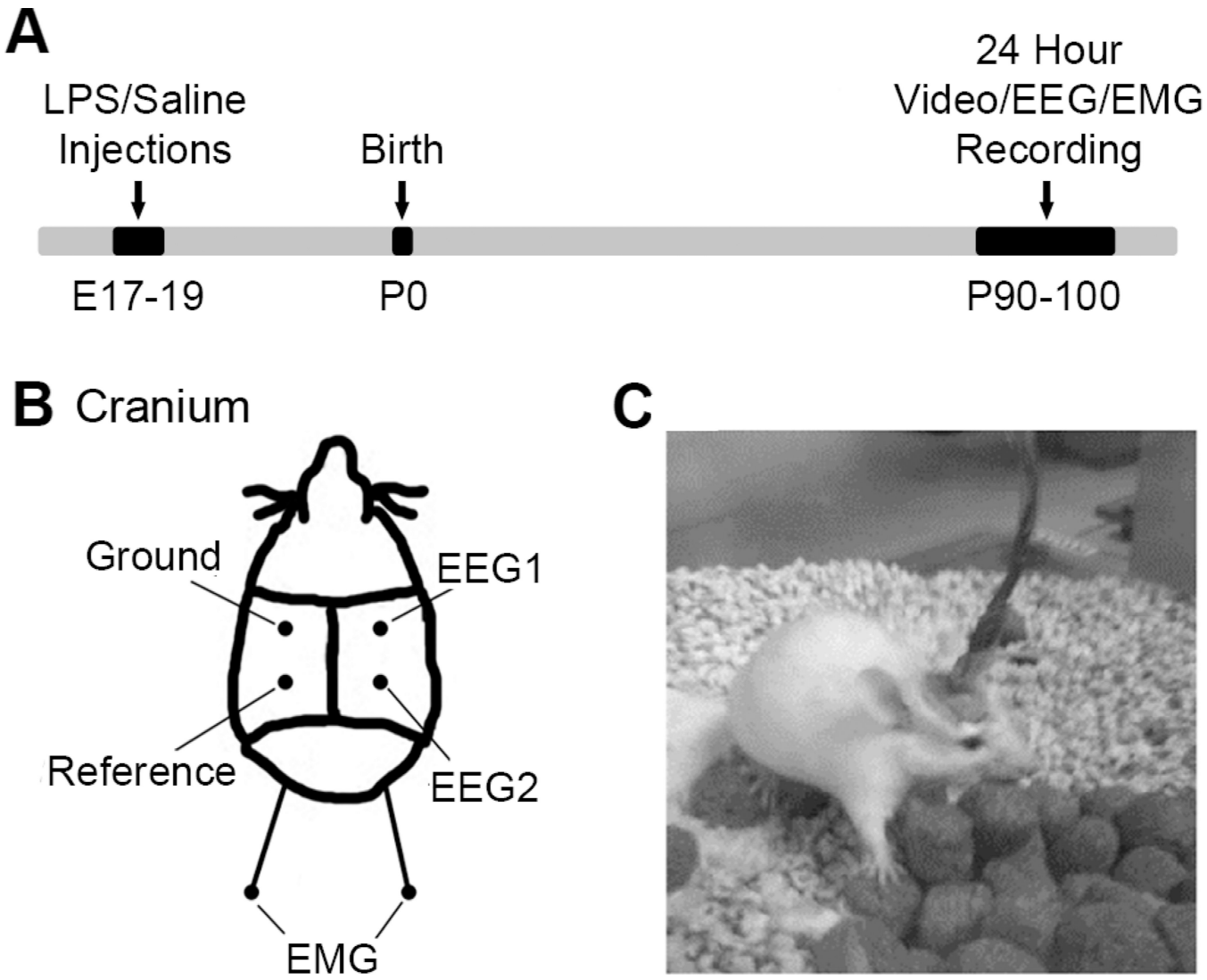

Figure 1. Schematic with experimental timeline and EEG placement

(A) The timeline of events starting with LPS/Saline injections at prenatal 17–19, to birth and recordings at post-natal 90–100. **(B)** The location of the EEG/EMG electrodes on each mouse's cranium. EEG1, EEG2, ground and reference subdural electrodes were placed parasagittally. In addition, two EMG electrodes were placed sub-dermally over supra scapular region. **(C)** A representative mouse during a tethered recording in recording chamber.

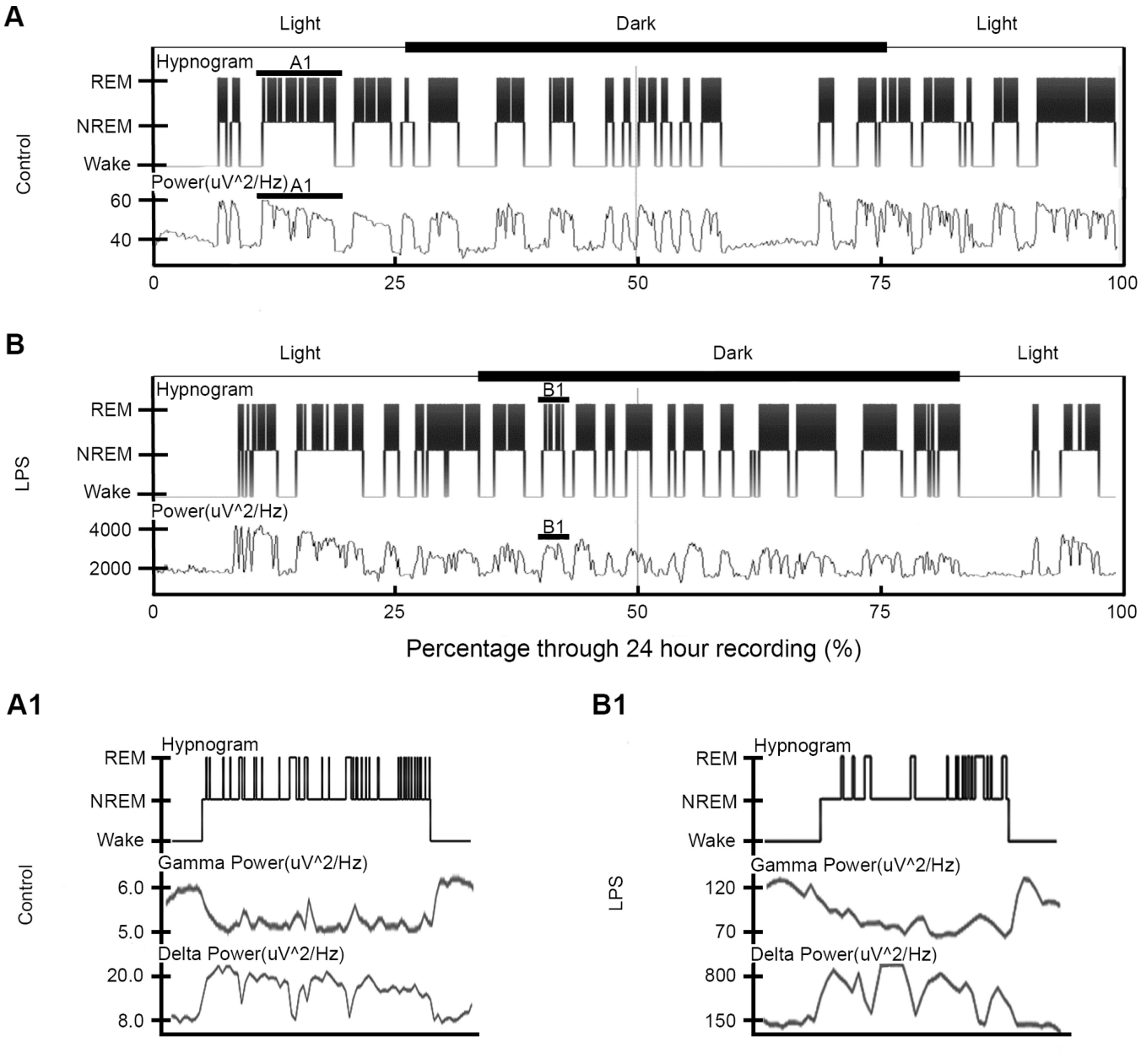

Figure 2. Hypnogram and power for control and LPS mouse over 24-hour period

(A) and **(B)** The hypnogram (top) and full EEG power spectrum (bottom) for one control and LPS mouse respectively as a graph of sleep state vs. percentage through recording. All power data is in units of uV^2/Hz. The y-axis depicted wake and sleep states for the power spectrum of each mouse, while the hypnogram is split into wake, NREM and REM cycles. In addition, the axes above the hypnograms showed the timing of light and dark cycles during the recordings for each mouse. For both the control and LPS mice, a solid line highlighted one sleep cycle. These sleep cycles were enlarged in **(A1)** and **(B1)** corresponding to control and LPS respectively. The expansion showed the multiple REM cycles on the hypnograms per sleep cycle. Below the hypnograms was an example of the

gamma and delta power during that respective sleep cycle. Note the downward u-shape for the gamma power and the opposite shape for the delta power during the cycle.

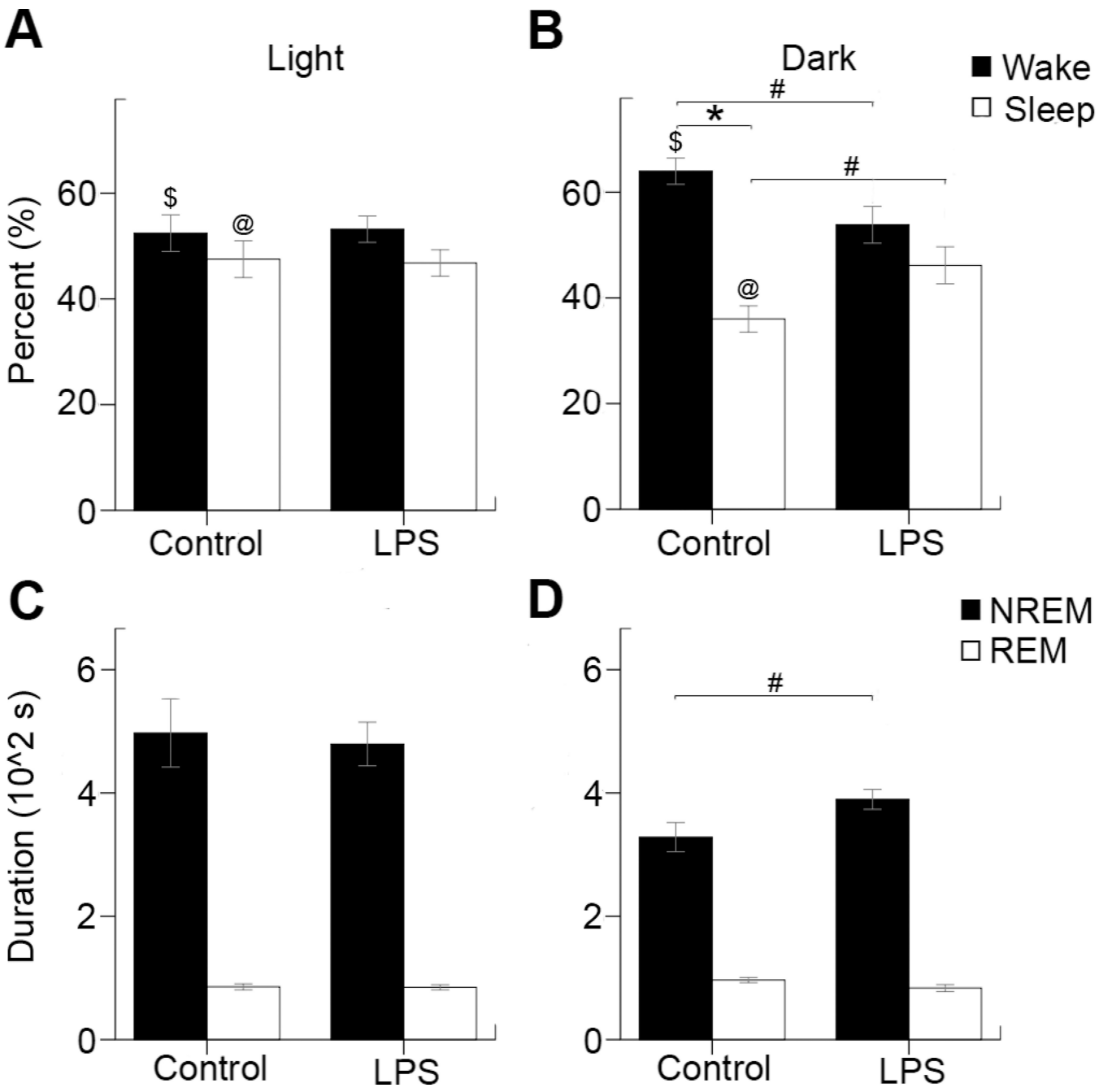

Figure 3. Circadian rhythm dependent sleep analysis for average time spent in sleep/wake states during the light and dark phase

(**A)** During the light cycle the control mice spent similar amount of time in wake (52±4%) and sleep (48±3%) states and LPS mice showed no significant differences [wake (53±2%) and sleep (47±2%) for LPS] **(B)** However in the dark cycle the control mice spent significantly more time awake (nocturnal animals) with wake (64±2%) and sleep (36±2%) compared to LPS mice where this diurnal variation was lost [wake (54±3%) and sleep (46±3%)]. **(C)** The average cycle duration of NREM (497±55sec) and REM (86±5sec) cycles for control mice, and NREM (479±35sec) and REM (85±4sec) for LPS mice during

the light cycle. **(D)** The average cycle duration of NREM (328±24sec) and REM (96±4sec) for control mice, and NREM (390±16sec) and REM (84±6sec) for LPS mice during the dark cycle. Statistical significance was determined by independent samples T-tests (#=$p<0.05$, n=18), and paired samples T-tests ($, @, *=$p<0.05$, n=8 control, n=10 LPS) within groups.

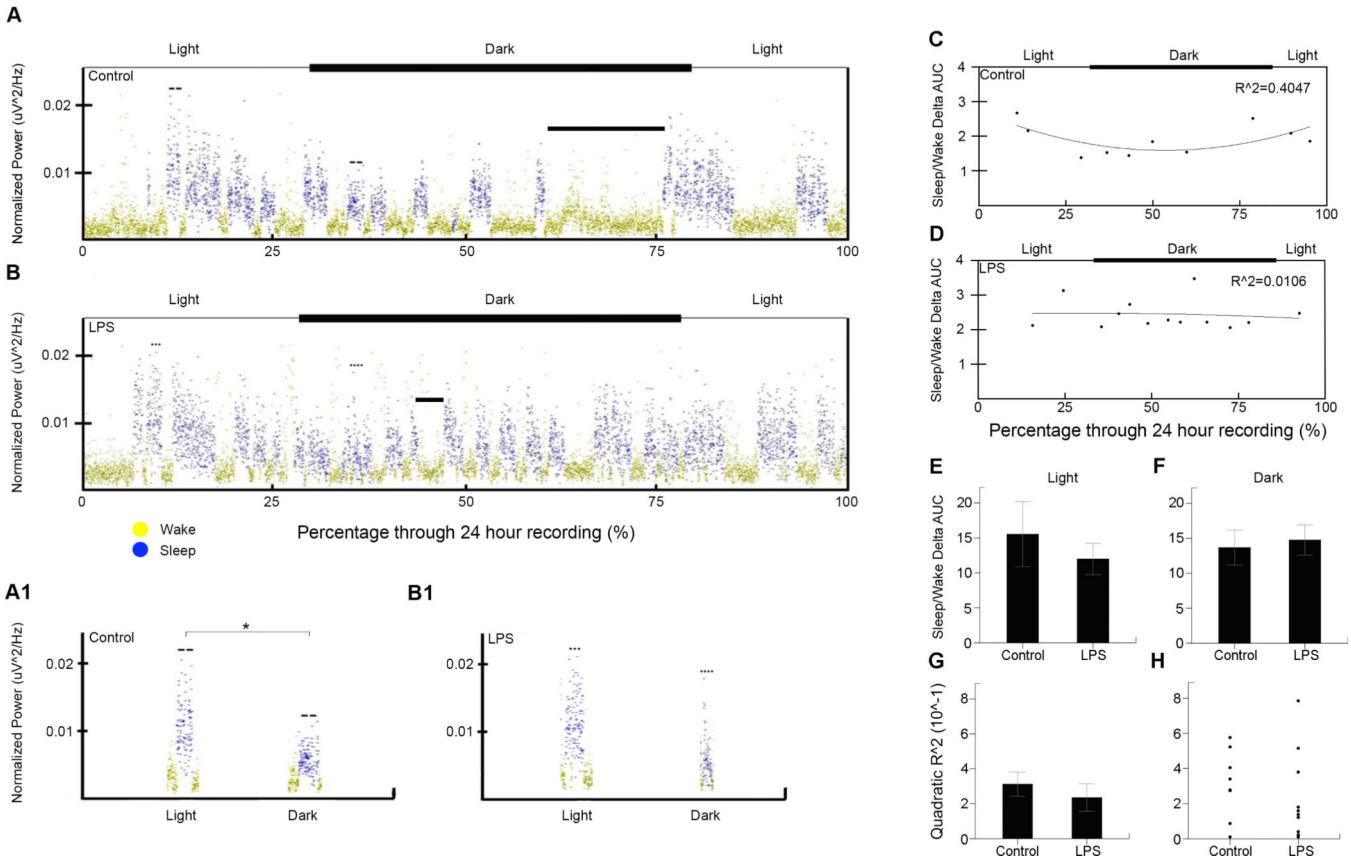

Figure 4. Delta power sleep/wake transition area under the curve (AUC) analysis

(A) and **(B)** the delta power vs. recording duration for a control and LPS mouse respectively. In addition, the axes above the delta power show the timing of light and dark cycles during the recordings for each mouse. Solid bars mark the nesting cycles of each mouse. **(A1)** and **(B1)** example sleep cycles from the light and dark cycles for a control and LPS mice respectively. The greater significance (*) is marked in **(A1)** reflecting the quadratic trend of control delta power over the circadian cycle. **(C)** and **(D)** Plot of sleep/wake delta power AUC ratios vs. percentage through recording for one control and LPS mouse respectively with fitted quadratic curve and R^2 value (control=0.40, LPS=0.01). Each point represents the ratio between the delta power AUC from the first ten minutes of sleep, and the previous ten minutes of wake. In addition, the axes above the hypnograms show the timing of light and dark cycles during the recordings for each mouse. **(E)** The ratio of sleep/wake delta power area under the curve (AUC) during ten-minute sleep, wake transition windows (ten-minute wake and ten-minute sleep) for the light cycle with controls (16±5) compared to LPS (12±2). **(F)** The ratio of sleep/wake delta power AUC during ten-minute transition windows for the dark cycle with controls (14±3) compared to LPS (15±2). **(G)** The quadratic coefficient of determination (R^2) for the sleep/wake AUC ratios for control (0.35±0.079) and LPS (0.23±0.079) mice. **(H)** Scatter plot showing spread of quadratic R^2 values for all control and LPS mice

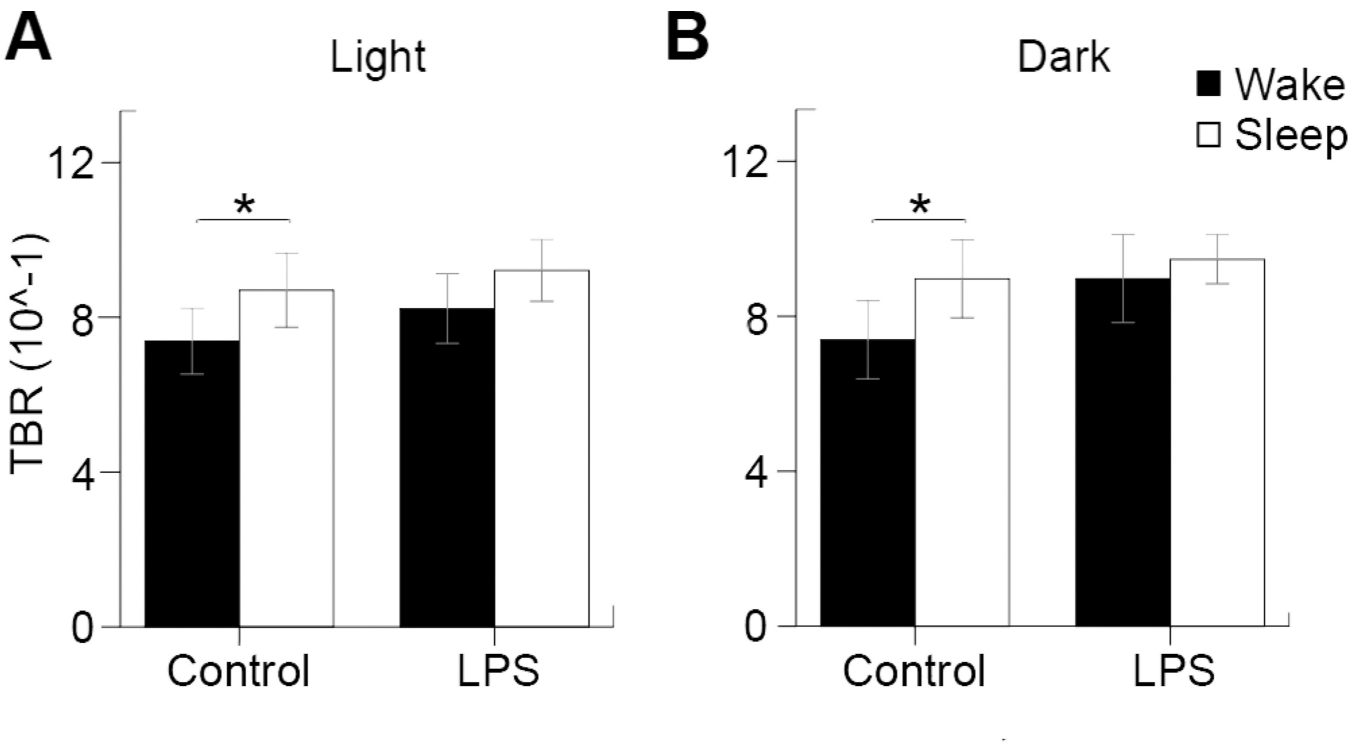

Figure 5. Theta-beta ratio analysis

(A) The theta-beta ratios for controls during wake (0.74±0.085) and sleep (0.87±0.096), as well as LPS during wake (0.82±0.010) and sleep (0.92±0.080) during the light cycle. **(B)** The theta-beta ratios for controls during wake (0.74±0.10) and sleep (0.90±0.10), as well as LPS during wake (0.90±0.11) and sleep (0.95±0.063) during the dark cycle. Statistical significance was determined by paired-samples T-tests (*=$p<0.05$, n=8 control, n=10 LPS).

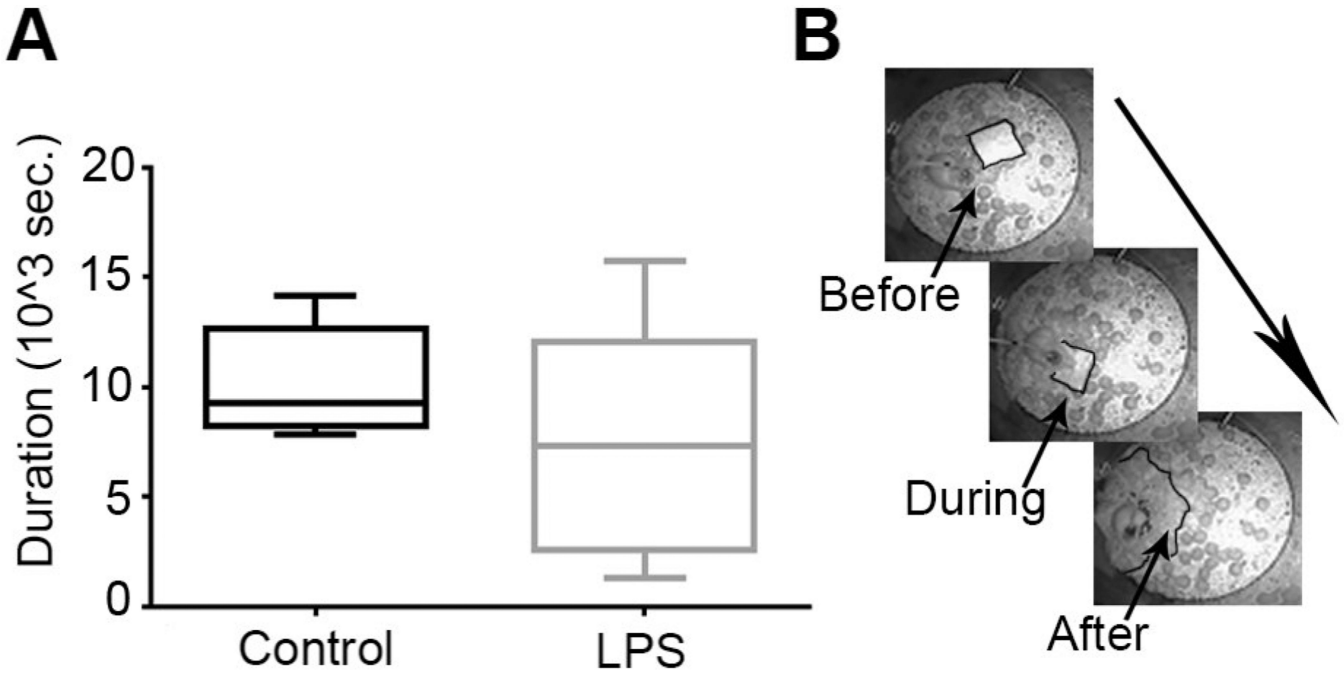

Figure 6. Nesting Cycle

(A) Boxplot describing the nesting cycle duration for control and LPS. **(B)** An example of the nesting cycle for one control mouse before, during and after the cycle respectively.